Tunable effective nonlinear refractive index of graphene dispersions during the distortion of spatial self-phase modulation

Gaozhong Wang, Saifeng Zhang, Fadhil A. Umran, Xin Cheng, Ningning Dong, Darragh Coghlan, Ya Cheng, Long Zhang, Werner J. Blau, and Jun Wang

Citation: Applied Physics Letters **104**, 141909 (2014); doi: 10.1063/1.4871092
View online: http://dx.doi.org/10.1063/1.4871092
View Table of Contents: http://scitation.aip.org/content/aip/journal/apl/104/14?ver=pdfcov
Published by the AIP Publishing

Tunable effective nonlinear refractive index of graphene dispersions during the distortion of spatial self-phase modulation

Gaozhong Wang,[1] Saifeng Zhang,[1,a)] Fadhil A. Umran,[2,3] Xin Cheng,[1] Ningning Dong,[1] Darragh Coghlan,[1,4] Ya Cheng,[2] Long Zhang,[1] Werner J. Blau,[1,4] and Jun Wang[1,a)]
[1]*Key Laboratory of Materials for High-Power Laser, Shanghai Institute of Optics and Fine Mechanics, Chinese Academy of Sciences, Shanghai 201800, China*
[2]*State Key Laboratory of High Field Laser Physics, Shanghai Institute of Optics and Fine Mechanics, Chinese Academy of Sciences, Shanghai 201800, China*
[3]*Institute of Laser for Post Graduate Studies, Baghdad University, Baghdad, Iraq*
[4]*School of Physics and the Centre for Research on Adaptive Nanostructures and Nanodevices (CRANN), Trinity College Dublin, Dublin 2, Ireland*

(Received 27 February 2014; accepted 31 March 2014; published online 9 April 2014)

Spatial self-phase modulation (SSPM) was observed directly when a focused He-Ne laser beam at 633 nm went through liquid-phase-exfoliated graphene dispersions. The diffraction pattern of SSPM was found to be distorted rapidly right after the incident beam horizontally passing through the dispersions, while no distortion for the vertically incident geometry. We show that the distortion is originated mainly from the non-axis-symmetrical thermal convections of the graphene nanosheets induced by laser heating, and the relative change of nonlinear refractive index can be determined by the ratio of the distortion angle to the half-cone angle. Therefore, the effective nonlinear refractive index of graphene dispersions can be tuned by changing the incident intensity and the temperature of the dispersions. © *2014 AIP Publishing LLC*. [http://dx.doi.org/10.1063/1.4871092]

Graphene possesses not only remarkable mechanical[1] and thermal properties[2] but also unique electronic[3] and photonic properties.[4] The electrons near the Dirac point in graphene have a linear dispersion between energy and momentum,[5] resulting in a continuously resonant optical response over a broad spectral region from the visible to the near-infrared.[6] Owing to the strong interband π-π^* electron transitions, graphene has a large effective third-order nonlinear susceptibility $\chi^{(3)}$, which has been confirmed by four-wave mixing[7] and Z-scan experiments.[6,8] Recently, Wu *et al.* reported the characterization of $\chi^{(3)}$ for chemically exfoliated graphene nanosheets using spatial self-phase modulation (SSPM),[9] a nonlinear optical phenomenon widely observed in optical materials and nanomaterials.[1,10,11] However, the SSPM pattern was not stable, and it was distorted in a short time, which, in general, is considered as a shortcoming for characterizing $\chi^{(3)}$ of nonlinear materials. The distortion phenomenon of SSPM has been reported in lots of nonlinear materials, such as liquid crystals,[12] carbon nanotubes,[13] and dye solutions.[14] It is ambiguously attributed to the thermal effect induced by the traversing laser beam. Ji *et al.* found the gravitation dependence of SSPM in carbon nanotube suspensions and estimated the change of the nonlinear refraction due to the gravity.[13] However, it is still unclear whether the distortion is dominated by the thermal convection of suspension[14] or the generation of bubbles in solvent.[9] In this work, we show that the distortion of SSPM pattern in graphene dispersions is originated from the non-axis-symmetrical thermal convections induced by laser heating. The half-cone angle of the diffraction patterns is independent on the linear refraction of the graphene dispersions and is only proportional to the effective nonlinear refractive index of the dispersions. Confirmed by the pressure experiment, the generation of solvent bubbles is tiny and can be neglected within our incident laser power range. We also estimated the relative change of effective nonlinear refractive index $\Delta n_{2e}/n_{2e}$, which could span from ~0.14 to ~0.375 by tuning the incident intensity or the temperature of the dispersions. The maximum change of the effective refractive index, i.e., $\Delta n_e = \Delta n_{2e} I$, can be up to ~0.05. The significant tunability of the effective nonlinear refractive index of the graphene dispersions manifests its potential applications in optical switching,[4] optical phase modulation,[15] optical limiting,[6,16,17] etc.

The graphene dispersions in N-methyl-2-pyrrolidone (NMP) were prepared using liquid phase exfoliation technique.[18] Different from the chemical exfoliation method,[19] the liquid exfoliation does not use any high-residual chemicals or ions, which could result in a change of the physical and chemical properties of the exfoliated graphene nanosheets,[18] and thus can largely guarantee high quality of the graphene used in the experiments. Owing to the nonlinear SSPM effect, a series of concentric rings can be observed after a focused cw He-Ne (633 nm) laser beam transmitting the graphene dispersions. The third-order susceptibility of graphene monolayer can be determined directly from the diffraction rings patterns.[9] In this experiment, it was found that the diffraction rings pattern was distorted rapidly after the incident laser beam horizontally passing through the graphene dispersions (see Figs. 1(a)–1(c)). As shown in Fig. 1(b), the initial diffraction pattern is nearly perfect concentric circles right after the horizontal incidence of the laser beam. In the subsequent few seconds, the upper half of the diffraction rings was collapsed to the center of the patterns, while the lower half retained the same (see Fig. 1(c)). Figure 1(d), in which diameters of the SSPM patterns along the two

a)Authors to whom correspondence should be addressed. Electronic addresses: sfzhang@siom.ac.cn and jwang@siom.ac.cn

orthogonal directions are depicted as functions of time, shows a dramatic reduction of the diameter in the vertical direction after it increases to a maximum in 0.32 s. In contrast, the diameter in the horizontal direction decreases slightly after the maximum. On the other hand, the laser beam was designed to be incident at the graphene dispersions along the vertical direction, as shown in Fig. 1(e). Under this geometry, the SSPM patterns retain unchanged with time, i.e., the collapse and deformation do not appear any more (see Figs. 1(f) and 1(g)). Figure 1(h) shows the diameters along the two orthogonal directions follow the same trend.

The SSPM is induced by the change of the intensity-dependent effective refractive index of graphene dispersions, which is expressed as $n_e = n_{0e} + In_{2e}$,[9,12] where n_{0e} and n_{2e} are the effective linear and nonlinear refractive index, respectively, and I is the incident laser intensity. Thus, the distortion of the SSPM patterns should result from the change of n_{0e} and/or n_{2e}. Hereinafter, we demonstrate that the change of n_{2e} dominates the distortion, rather than that of n_{0e}.

The change of n_{0e} of the graphene dispersions is mainly from two possibilities: The possible solvent bubbles induced by laser heating and the concentration variation of graphene caused by thermal convection. The following pressure experiment confirms that the change of n_{0e} resulting from solvent bubbles can be neglected. In the experiment, a cuvette with the graphene dispersions was placed in a vacuum chamber, the pressure of which can be controlled by a mechanical pump.[20] The relationship between the bubble size r_B and the air pressure P can be estimated approximately by the equation[6]

$$2\gamma = \frac{3MRT}{4\pi r_B^2} - Pr_B, \tag{1}$$

where γ is the surface tension, M is the number of moles of gas, R is the universal gas constant, and T is the absolute temperature in the bubbles. From Eq. (1), bubble size as a function of atmospheric pressure can be deduced. As illustrated in Fig. 2(a), the bubble can increase dramatically when the pressure decreases nearly to zero. For instance, when the vacuum pressure changes from 1.00 atm to 0.02 atm, the calculated bubble size r_B can increase from 0.835 μm to 2.95 μm (M was assumed to be 1.0×10^{-16} mol). The volume of the bubbles becomes 44 times greater, implying that a large variation of n_{0e} of the graphene dispersions occurs and the distortion pattern should change dramatically if n_{0e} dominates the process. However, from Fig. 2(b), it can be seen that the distortion time, distortion angle, and half-cone angle keep stable when the air pressure decreases from 1.00 atm to 0.02 atm in the experiment. The results indicate that the change of n_{0e} resulting from solvent bubbles is negligible within our incident laser power range (0–54 W/cm^2).

The change of effective linear refractive index Δn_{0e} of the graphene dispersions caused by thermal convection is also very tiny. Suppose the graphene nanosheets can be completely depleted during thermal convection, Δn_{0e} should be the maximum. It is noticed that the thickness of graphene nanosheets is much smaller than the irradiation wavelength and the observed scattering induced by the lateral size is also negligible. Therefore, Bruggeman effective medium theory is applicable to calculate the effective refractive index n_{0e} of the graphene dispersions,[21–23] by considering the refractive index and volume fraction of each composition

$$\eta_{NMP}\frac{n_{\mathrm{NMP}}^2 - n_{0e}^2}{n_{\mathrm{NMP}}^2 + 2n_{0e}^2} + \eta_G\frac{n_{\mathrm{G}}^2 - n_{0e}^2}{n_{\mathrm{G}}^2 + 2n_{0e}^2} = 0, \tag{2}$$

where $n_{NMP} = 1.47$ and $n_G = 2.60$ are the linear refractive indices of NMP and graphene, respectively.[24,25] η_G and η_{NMP} are the volume fractions of graphene and NMP in the dispersion, respectively ($\eta_G + \eta_{NMP} = 1$). Here, we consider only

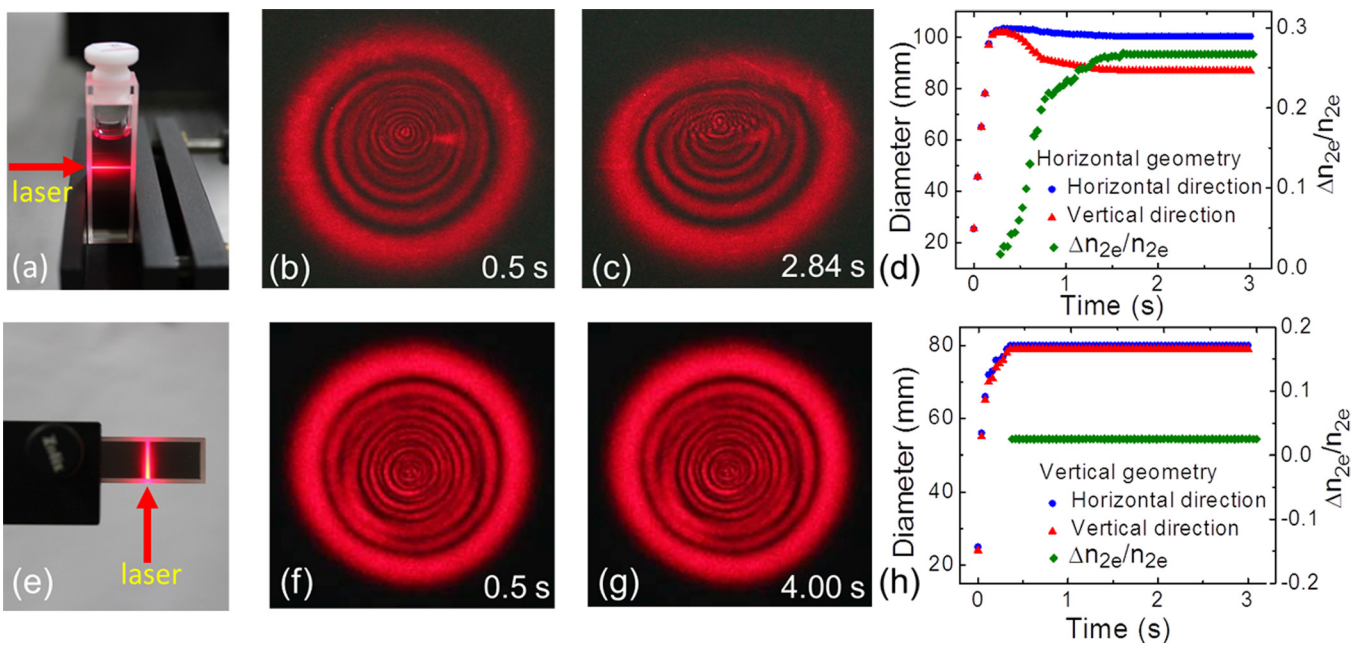

FIG. 1. (a) The horizontally incident geometry of the SSPM experiment. (b) An initial SSPM diffraction ring pattern and (c) the distorted pattern. (d) Diameters of the outermost ring along the horizontal and vertical directions and $\Delta n_{2e}/n_{2e}$ as functions of time. (e)–(h) The vertically incident case. (Multimedia view) [URL: http://dx.doi.org/10.1063/1.4871092.1] [URL: http://dx.doi.org/10.1063/1.4871092.2]

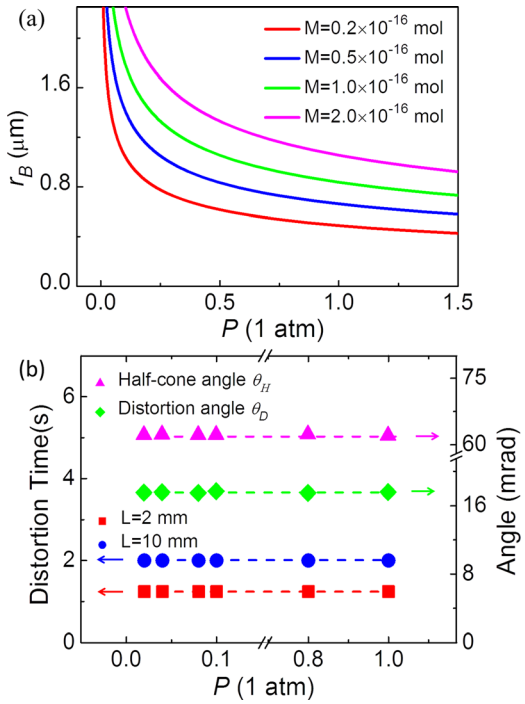

FIG. 2. (a) Bubble size as a function of atmospheric pressure P. (b) The distortion time, distortion angle, and half-cone angle as functions of P. L is the thickness of the quartz cuvette.

the change of n_{0e} of the graphene dispersions within the quasi-cylinder volume of the incident laser beam. The hyperbolic shape of the focused laser beam has less of an influence on the result. Therefore, η_G can be estimated by

$$\eta_G = \frac{N_{eff} S d_{th}}{SL} = \frac{N_{eff} d_{th}}{L}, \tag{3}$$

where $N_{eff} \sim 48$ is the effective number of graphene monolayer, which can be estimated by $T_{monolayer}^{N_{eff}} = T_{total}$, where T_{total} is the transmittance of the graphene dispersions ($\sim$32.72% at 633 nm), and $T_{monolayer} \sim 97.7\%$ is the transmittance of graphene monolayer.[9,26] S is the cross sectional area of laser beam, $d_{th} = 0.335$ nm is the thickness of graphene monolayer,[27] and $L = 10$ mm is the thickness of quartz cuvette. According to Eqs. (2) and (3), the n_{0e} is calculated to be $(0.98 \times 10^{-6}) n_{NMP}$, meaning that the order of magnitude of the change of n_{0e} caused by thermal convection of the graphene nanosheets in NMP while irradiated by a cw He-Ne laser should be smaller than $10^{-6} n_{NMP}$. Thus, the contribution of n_{0e} to the distortion of SSPM pattern can be ignored in this work.

The carriers within graphene nanosheets response in phase in the light field while constructing the SSPM ring patterns according to the theory of Wu *et al.*[9] Although the top half of the diffraction pattern distorts to a smaller amplitude, the interference pattern can be seen in Fig. 1(c), implying that the coherent response induced by graphene still remains. As we discussed above, the smaller amplitude of the interference pattern is largely induced by the change of effective nonlinear refractive index n_{2e} of the graphene dispersions, resulting from the variation of local graphene nanosheets concentration caused by the non-axis-symmetrical thermal convections.[14,28] Indeed, the diffraction ring diameter of the graphene dispersions was decreased when the concentration of graphene nanosheets was reduced, as shown in Fig. 3(a).

In the following part, we show theoretically that the half-cone angle of the diffraction pattern is only proportional to n_{2e} and is independent on n_{0e}. As a result, the change of n_{2e} can be estimated by studying the distortion dynamics. As illustrated in the inset of Fig. 3(c), we define θ_D as the distortion angle to measure the degree of distortion for the SSPM patterns and define θ_H as the half-cone angle. The half-cone angle of the diffraction ring can be expressed as[12]

$$\theta_H \approx \frac{\lambda}{2\pi} \left(\frac{d\Delta\psi}{dr} \right)_{max}, \tag{4}$$

where $\Delta\psi(r) = (\frac{2\pi}{\lambda}) \int_0^L n_{2e} I(r,z) dz$ is the corresponding phase shift of the laser beam after traversing the graphene dispersions with the effective pathlength of L. λ is the wavelength of the laser, r is the transverse position in the beam. For a Gaussian beam, Eq. (4) can be rewritten in a compact form of

$$\theta_H \approx n_{2e} C, \tag{5}$$

where $C = [-\frac{8IrL}{w_0^2} \exp(-\frac{2r^2}{w_0^2})]_{max}$, $r \in [0, +\infty)$ is a constant. Equation (5) implies that the half-cone angle θ_H is only proportional to the effective nonlinear refractive index n_{2e} and is independent on n_{0e}. According to Eq. (5), Δn_{2e}, the change of n_{2e} before and after the distortion, can be deduced in the form of

$$\Delta n_{2e} / n_{2e} = \theta_D / \theta_H, \tag{6}$$

where θ_D and θ_H can be measured readily at different intensities in the experiment. As shown in Fig. 3(b), θ_D as well as θ_H increases quasi-linearly as the incident intensity increases, implying a more severe distortion of the patterns at the higher intensities. Figure 3(c) gives the deduced $\Delta n_{2e}/n_{2e}$, which increases from 14% to 28% when the incident intensity increases from 17.3 to 54.0 W/cm^2.

From Eq. (6), we can directly see that the distortion originates from the change of n_{2e}, which is ascribed to the laser induced thermal convections,[9,14] rather than the change of n_{0e}. The convection induced by laser beam is analogous to the onset of convection near a suddenly heated horizontal wire, which was investigated in details by Vest and Lawson.[28] Since graphene possesses high thermal conductivity and optical absorption coefficient,[5,26] the dispersions can be effectively heated by the incident cw laser beam and the temperature gradient along the vertical direction arises, resulting in strong thermal convections near the focus in the dispersions, as illustrated in the inset of Fig. 3(d). Density of graphene nanosheets in the upper part of the beam becomes less dense when strong convections occur, resulting in a reduction of the effective nonlinear refractive index.[28] According to Ref. 9, the total third-order nonlinear susceptibility $\chi_{total}^{(3)} \approx N_{eff}^2 \chi_{monolayer}^{(3)}$. When the local concentration of graphene dispersions in the laser beam changes, N_{eff} and hence $\chi_{total}^{(3)}$ will be changed correspondingly. As $\chi_{total}^{(3)}$ is proportional to the effective nonlinear refractive index n_{2e}, $n_{2e} = (1.2 \times 10^4 \times \pi^2 / n_0^2 c) \chi_{total}^{(3)}$, n_{2e} can then be tuned by

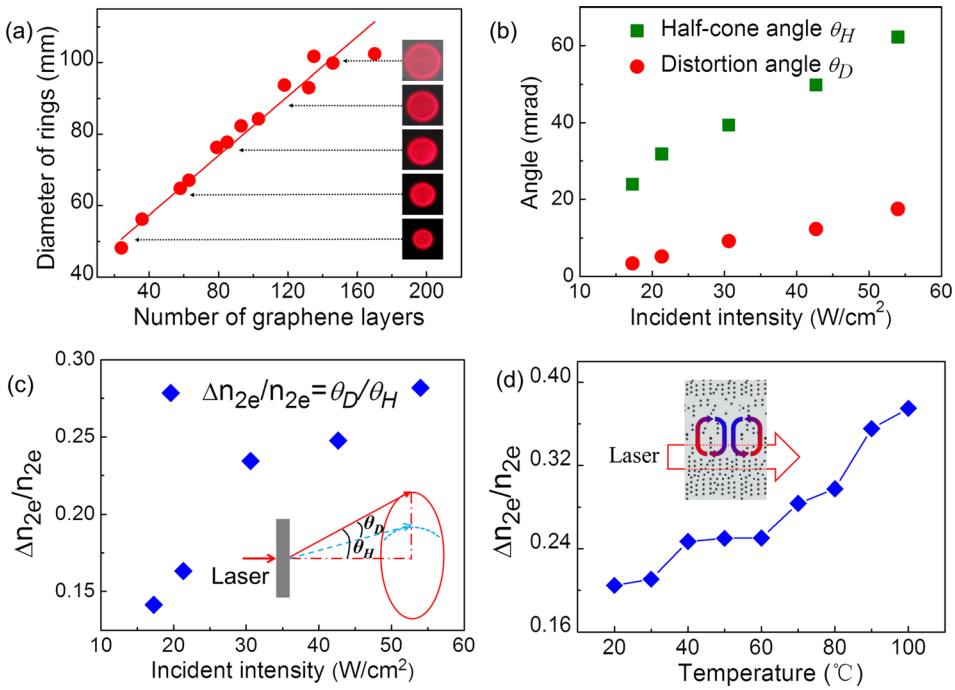

FIG. 3. (a) Diameter of outermost diffraction ring as a function of effective number of graphene monolayers. Inset: Photographs of the corresponding SPM patterns. (b) Distortion angle θ_D, half-cone angle θ_H, and (c) $\Delta n_{2e}/n_{2e}$ as functions of incident intensity. Inset: Illustration of the distortion angle and half-cone angle. (d) $\Delta n_{2e}/n_{2e}$ versus temperature of the graphene dispersions. Inset: Illustration of the thermal convections in the graphene dispersions by laser heating.

the change of graphene concentration caused by the thermal convection. Half of the laser beam is diffracted by the dispersions with reduced n_{2e}, leading to the upper part of the diffraction rings distorting to the center of the patterns. On the contrary, the non-axis-symmetrical thermal convection is eliminated in the vertical incident geometry and the distortion phenomenon disappears, as shown in Fig. 1(g). The variation of $\Delta n_{2e}/n_{2e}$ with time is also calculated and depicted in Figs. 1(d) and 1(h) for the two incident geometries.

In addition, we measured the distortion angle and half-cone angle of the SPM patterns at different temperatures. As shown in Fig. 3(d), when the temperature of the graphene dispersions increases from 20 °C to 100 °C, $\Delta n_{2e}/n_{2e}$ is ~20% at 20 °C and increases gradually to ~37.5% at 100 °C. n_{2e} of the graphene dispersions can be calculated via the relation between the diffraction ring number and the incident intensity,[9] and it is 1.13×10^{-5} cm^2/W in our experiment. Thus, Δn_e can be tuned up to 0.05 ($\Delta n_{2e}/n_{2e} = 0.375$) when N_{eff} is set to 700, larger than carrier induced one (~0.01) in InP, GaAs, InGaAsP[29] and electric field induced one (~0.01) in some organic materials, say, ATOP dyes.[30]

In summary, we show that the distortion of the diffraction rings patterns in the horizontal incident geometry, while eliminated in the vertical one, is mainly attributed to the change of local graphene nanosheets concentration induced by the non-axis-symmetrical thermal convections. The relative change of local nonlinear refractive index $\Delta n_{2e}/n_{2e}$ can be obtained directly by measuring the distortion angle and half-cone angle. Tuned by the incident intensity and dispersion temperature, the relative change of the effective refractive index of graphene dispersions $\Delta n_{2e}/n_{2e}$ can be spanned from ~0.14 to ~0.375, implying potential applications in nonlinear optical modulation devices.

J.W. thanks the financial supports from the National 10000-Talent Program, CAS 100-Talent Program, NSFC (No. 61178007), STCSM Nano Project 11nm0502400, and Shanghai Pujiang Program 12PJ1409400. S.F.Z. thanks the STCSM (No. 12ZR1451800) and NSFC (No. 61308034). N.N.D. thanks the China Postdoctoral Science Foundation (2012M520049) and NSFC (No. 61308087). L.Z. thanks the financial supports from NSFC (No. 51072207) and STCSM (No. 10XD1404600). W.J.B. gratefully acknowledges the China National High-end Foreign Experts Program (No. GDJ20130491010) and Science Foundation Ireland (SFI, 12/IA/1306).

[1]C. Lee, X. D. Wei, J. W. Kysar, and J. Hone, Science **321**, 385 (2008).
[2]A. A. Balandin, S. Ghosh, W. Z. Bao, I. Calizo, D. Teweldebrhan, F. Miao, and C. N. Lau, Nano Lett. **8**, 902 (2008).
[3]K. S. Kim, Y. Zhao, H. Jang, S. Y. Lee, J. M. Kim, K. S. Kim, J. H. Ahn, P. Kim, J. Y. Choi, and B. H. Hong, Nature **457**, 706 (2009).
[4]F. Bonaccorso, Z. Sun, T. Hasan, and A. C. Ferrari, Nat. Photonics **4**, 611 (2010).
[5]A. K. Geim and K. S. Novoselov, Nature Mater. **6**, 183 (2007).
[6]J. Wang, Y. Hernandez, M. Lotya, J. N. Coleman, and W. J. Blau, Adv. Mater. **21**, 2430 (2009).
[7]E. Hendry, P. J. Hale, J. Moger, A. K. Savchenko, and S. A. Mikhailov, Phys. Rev. Lett. **105**, 097401 (2010).
[8]H. Zhang, S. Virally, Q. L. Bao, L. K. Ping, S. Massar, N. Godbout, and P. Kockaert, Opt. Lett. **37**, 1856 (2012).
[9]R. Wu, Y. L. Zhang, S. C. Yan, F. Bian, W. L. Wang, X. D. Bai, X. H. Lu, J. M. Zhao, and E. G. Wang, Nano Lett. **11**, 5159 (2011).
[10]M. Horowitz, R. Daisy, O. Werner, and B. Fischer, Opt. Lett. **17**, 475 (1992).
[11]F. Bloisi, L. Vicari, F. Simoni, G. Cipparrone, and C. Umeton, J. Opt. Soc. Am. B **5**, 2462 (1988).
[12]S. D. Durbin, S. M. Arakelian, and Y. R. Shen, Opt. Lett. **6**, 411 (1981), available at http://www.opticsinfobase.org/ol/abstract.cfm?uri=ol-6-9-411.
[13]W. Ji, W. Chen, S. Lim, J. Lin, and Z. Guo, Opt. Express **14**, 8958 (2006).
[14]R. Karimzadeh, J. Opt. **14**, 095701 (2012).
[15]N. Konforti, E. Marom, and S.-T. Wu, Opt. Lett. **13**, 251 (1988).
[16]Y. Xu, Z. Liu, X. Zhang, Y. Wang, J. Tian, Y. Huang, Y. Ma, X. Zhang, and Y. Chen, Adv. Mater. **21**, 1275 (2009).
[17]Y. Zhou, Q. Bao, L. A. L. Tang, Y. Zhong, and K. P. Loh, Chem. Mater. **21**, 2950 (2009).
[18]Y. Hernandez, V. Nicolosi, M. Lotya, F. M. Blighe, Z. Y. Sun, S. De, I. T. McGovern, B. Holland, M. Byrne, Y. K. Gun'ko *et al.*, Nat. Nanotechnol. **3**, 563 (2008).
[19]C. Valles, C. Drummond, H. Saadaoui, C. A. Furtado, M. He, O. Roubeau, L. Ortolani, M. Monthioux, and A. Penicaud, J. Am. Chem. Soc. **130**, 15802 (2008).

[20]X. Cheng, N. Dong, B. Li, X. Zhang, S. Zhang, J. Jiao, W. J. Blau, L. Zhang, and J. Wang, Opt. Express **21**, 16486 (2013).
[21]G. A. Niklasson, C. G. Granqvist, and O. Hunderi, Appl. Opt. **20**, 26 (1981).
[22]W. T. Doyle, Phys. Rev. B **39**, 9852 (1989).
[23]F. J. Garcia-Vidal, J. M. Pitarke, and J. B. Pendry, Phys. Rev. Lett. **78**, 4289 (1997).
[24]S. Chen, W. Fang, J. Yao, and H. Zong, J. Chem. Eng. Data **46**, 596 (2001).
[25]Z. Ni, H. Wang, J. Kasim, H. Fan, T. Yu, Y. Wu, Y. Feng, and Z. Shen, Nano Lett. **7**, 2758 (2007).
[26]R. R. Nair, P. Blake, A. N. Grigorenko, K. S. Novoselov, T. J. Booth, T. Stauber, N. M. R. Peres, and A. K. Geim, Science **320**, 1308 (2008).
[27]Y. Huang, J. Wu, and K. C. Hwang, Phys. Rev. B **74**, 245413 (2006).
[28]C. M. Vest and M. L. Lawson, Int. J. Heat Mass Transfer **15**, 1281 (1972).
[29]B. R. Bennett, R. A. Soref, and J. A. Delalamo, IEEE J. Quantum Electron. **26**, 113 (1990).
[30]F. Wurthner, S. Yao, J. Schilling, R. Wortmann, M. Redi-Abshiro, E. Mecher, F. Gallego-Gomez, and K. Meerholz, J. Am. Chem. Soc. **123**, 2810 (2001).